

1 BBA - Proteins and Proteomics

2

3 **Thermodynamic analysis of ionizable groups involved in the catalytic mechanism**  
4 **of human matrix metalloproteinase 7 (MMP-7)**

5

6 Hitoshi Takeharu, Kiyoshi Yasukawa, Kuniyo Inouye\*

7

8 *Division of Food Science and Biotechnology, Graduate School of Agriculture, Kyoto*  
9 *University, Sakyo-ku, Kyoto 606-8502, Japan*

10

11 *Abbreviations:* AMPSO, 3-[(1,1-dimethyl-2-hydroxy-ethyl)amino]-2-  
12 hydroxypropane sulfonic acid; DMSO, dimethyl sulfoxide; HEPES,  
13 2-[4-(2-hydroxyethyl)-1-piperazinyl] ethanesulfonic acid;  $K_e$ , proton dissociation  
14 constant; MES, 2-(*N*-morpholino)ethanesulfonic acid; MMP, matrix metalloproteinase;  
15 MOCAc-PLG, (7-methoxycoumarin-4-yl)acetyl-L-Pro-L-Leu-Gly; MOCAc-  
16 PLGL(Dpa)AR, (7-methoxycoumarin-4-yl)acetyl-L-Pro-L-Leu-Gly-L-Leu-[*N*<sup>3</sup>-(2,4-  
17 dinitrophenyl)-L-2,3-diaminopropionyl]-L-Ala-L-Arg-NH<sub>2</sub>.

18 \*Correspondence author. Tel.: +81 75 753 6266; fax: +81 75 753 6265. *E-mail*  
19 *address:* inouye@kais.kyoto-u.ac.jp

20 *Keywords:* ionizable group; matrix metalloproteinase; MMP-7; proton dissociation  
21 constant; thermodynamic analysis.

22

23

24

25 **Abstract**

26

27 Human matrix metalloproteinase 7 (MMP-7) exhibits a broad bell-shaped  
28 pH-dependence with the acidic and alkaline  $pK_e$  ( $pK_{e1}$  and  $pK_{e2}$ ) values of about 4 and  
29 10. In this study, we estimated the ionizable groups involved in its catalytic mechanism  
30 by thermodynamic analysis.  $pK_a$  of side chains of L-Asp, L-Glu, L-His, L-Cys, L-Tyr,  
31 L-Lys, and L-Arg at 25-45°C were determined by the pH titration of amino-acid  
32 solutions, from which their enthalpy changes,  $\Delta H^\circ$ , of deprotonation were calculated.  
33  $pK_{e1}$  and  $pK_{e2}$  of MMP-7 at 15-45°C were determined in the hydrolysis of  
34 (7-methoxycoumarin-4-yl)acetyl-L-Pro-L-Leu-Gly-L-Leu-[ $N^3$ -(2,4-dinitrophenyl)-L-2,3-  
35 diaminopropionyl]-L-Ala-L-Arg-NH<sub>2</sub>, from which  $\Delta H^\circ$  for  $pK_{e1}$  and  $pK_{e2}$  were  
36 calculated. The  $\Delta H^\circ$  for  $pK_{e1}$  ( $-20.6 \pm 6.1 \text{ kJ mol}^{-1}$ ) was similar to that for L-Glu ( $-23.6 \pm$   
37  $5.8 \text{ kJ mol}^{-1}$ ), and the  $\Delta H^\circ$  for  $pK_{e2}$  ( $89.9 \pm 4.0 \text{ kJ mol}^{-1}$ ) was similar to those for L-Arg  
38 ( $87.6 \pm 5.5 \text{ kJ mol}^{-1}$ ) and L-Lys ( $70.4 \pm 4.4 \text{ kJ mol}^{-1}$ ). The mutation of the active-site  
39 residue Glu198 into Ala completely abolished the activity, suggesting that Glu198 is the  
40 ionizable group for  $pK_{e1}$ . On the other hand, no arginine or lysine residues are found in  
41 the active site of MMP-7. We proposed a possibility that a protein-bound water is the  
42 ionizable group for  $pK_{e2}$ .

43

44

45

## 46 **1. Introduction**

47

48 Human matrix metalloproteinase 7 (MMP-7, Matrilysin) [EC 3.4.24.23] is the  
49 smallest matrix metalloproteinase (MMP), lacking a carboxyl terminal hemopexin-like  
50 domain conserved in common MMPs. It is believed to play an important role in tumor  
51 invasion and metastasis [1, 2]. The molecular mass of the latent pro-form is 28 kDa, and  
52 that of its mature form is 19 kDa [3]. MMP-7 is composed of a five-stranded  $\beta$ -sheet  
53 and three  $\alpha$ -helices, and contains a zinc ion essential for activity and other zinc and  
54 calcium ions that are considered necessary for stability [4]. Like all other MMPs, it has  
55 the consensus sequence HEXXHXXGXXH, in which three histidine residues chelate a  
56 catalytic zinc ion, and a methionine-containing turn (Met-turn). Hence, it is grouped in  
57 clan MA(M) [5]. In recent years, target molecules through which MMP-7 exerts  
58 biological functions have become apparent, such as heparin [6], heparan sulfate [6],  
59 cholesterol sulfate [7-9], and ErbB4 receptor [10]. The inhibitions of MMP-7 activity by  
60 natural compounds [11,12], synthetic compounds [13], and detergents [14] were  
61 reported.

62 Generally, ionizable groups involved in the catalytic mechanisms of enzyme are  
63 estimated from the three-dimensional structure and  $pK_e$  values. Figure 1A shows the  
64 structure of MMP-7-hydroxamate inhibitor complex [4]. In this study, the numbering of  
65 amino acid residues of pro-MMP-7 is according to the previous report [15], in which the  
66 mature MMP-7 begins at Tyr78. MMP-7 has three  $\alpha$  helices and five  $\beta$  strands [4].  
67 Tyr193 and Glu198 are located at the second  $\alpha$ -helix (Leu192-Leu203), while Tyr216  
68 and Tyr219 are located at the Met-turn (Pro211-Gly222). Sequence comparison of  
69 MMP-1 [16], MMP-2 [17], MMP-3 [18], MMP-7 [19], MMP-8 [20], MMP-9 [21],

70 MMP-10 [19], MMP-11 [22], MMP-12 [21], MMP-13 [21], and MMP-14 [23] revealed  
71 that Glu198 and Tyr219 are conserved in all MMPs, while Tyr216 is conserved in  
72 several MMPs, and Tyr193 is unique to MMP-7 [24]. Tyr219 and Tyr216 form the S1'  
73 subsite. MMP-7 exhibits a broad bell-shaped pH-dependence with the acidic and  
74 alkaline  $pK_e$  ( $pK_{e1}$  and  $pK_{e2}$ ) values of about 4 and 10 [13,25]. As a result, three  
75 ionization forms of MMP-7 and MMP-7-substrate complex are considered, respectively  
76 (Fig. 2). Glu198 and Tyr219 are believed to be the ionizable groups responsible for  $pK_{e1}$   
77 and  $pK_{e2}$ , respectively. However, Cha *et al.* proposed that the zinc-bound water might be  
78 the ionizable group responsible for  $pK_{e1}$  [26]. We found that the MMP-7 whose tyrosyl  
79 residues were nitrated with tetranitromethane retained activity [27]. In addition, we  
80 recently demonstrated that all Tyr219 variants retained activity [28]. These results  
81 indicate that Tyr219 is not critical for catalytic activity. We also demonstrated that  
82 Tyr193 and Tyr216 variants retained activity [28].

83 One of the critical problems with using  $pK_a$  values of free amino acids for  
84 estimation of charge states of amino acid residues is that little water (and hence protons)  
85 is available for the residues buried in a protein core, while large amounts of water (55 M  
86 water) is available for the residues facing bulk solution. In 1930-1960, enthalpy changes,  
87  $\Delta H^\circ$ , of deprotonation of side chains of amino acid residues were determined by the  
88 measurement of pH- and temperature-dependences of electromotive force of the battery  
89 containing amino acids, dipeptides, or tripeptides in a cell [29-33]. It was demonstrated  
90 that in dipeptides and tripeptides,  $\Delta H^\circ$  values of side chains of amino acid residues are  
91 not affected by the amino acid residues in their neighborhoods and are almost equal to  
92 the  $\Delta H^\circ$  values of side chains of free amino acids [29-33]. Therefore,  $\Delta H^\circ$  values can be  
93 used as a clue to estimate the ionizable groups in the catalytic mechanism of enzymes

94 [29,34-36]. However, compared with the estimation of the ionizable groups with  $pK_e$   
95 values, the estimation with  $\Delta H^0$  values is not commonly used. This might be due to that  
96 reliable  $\Delta H^0$  values of side chains of amino acid residues have not been available. In this  
97 study, we determined the  $\Delta H^0$  of side chains of amino acid residues by the pH-titration  
98 of amino-acid solutions and used them to estimate the ionizable groups involved in the  
99 catalytic mechanism of MMP-7.

100

## 101 **2. Materials and methods**

102

### 103 *2.1. Materials*

104

105 (7-methoxycoumarin-4-yl)acetyl-L-Pro-L-Leu-Gly-L-Leu-[ $N^3$ -(2,4-dinitrophenyl)-  
106 L-2,3-diaminopropionyl]-L-Ala-L-Arg-NH<sub>2</sub> [MOCAc-PLGL(Dpa)AR] (Lot 491214,  
107 molecular mass 1093.2 Da) [37] and (7-methoxycoumarin-4-yl)acetyl-L-Pro-L-Leu-Gly  
108 (MOCAc-PLG) (Lot 510913, molecular mass 501.54 Da) were purchased from the  
109 Peptide Institute (Osaka, Japan). Their concentrations were determined by the denoted  
110 weight and the molecule weight.  
111 3-[(1,1-Dimethyl-2-hydroxy-ethyl)amino]-2-hydroxypropane sulfonic acid (AMPSO,  
112 Lot 9355C, molecular mass 227.3 Da) and L-Glu (Lot TLE5153) were from Wako Pure  
113 Chemical (Osaka). L-Asp (Lot 115H0563) and  $N^\alpha$ -acetyl-L-Lys (Lot A1020) were from  
114 Sigma (St. Louis, MO, USA). L-His (Lot M2N7937), L-Cys (Lot M7H2081), L-Tyr,  
115 (Lot M7K3391), and L-Arg (Lot M7K6540) were from Nacalai Tesque (Kyoto, Japan).  
116 All other chemicals were from Nacalai Tesque.

117

118 2.2. *Expression and purification of MMP-7*

119

120 Expression in *Escherichia coli* and purification of recombinant MMP-7 were  
121 carried out, as described previously [31,39]. Briefly, mature MMP-7 (Met77-Lys250)  
122 was expressed in BL21(DE3) cells in the forms of inclusion bodies, solubilized with 6  
123 M guanidine HCl, refolded with 1 M L-arginine, and purified by sequential ammonium  
124 sulfate precipitation and heparin affinity column-chromatography procedures of the  
125 refolded products. The concentration of MMP-7 was determined spectrophotometrically  
126 using the molar absorption coefficient at 280 nm,  $\epsilon_{280}$ , of 31,800 M<sup>-1</sup> cm<sup>-1</sup> [38].  
127 Site-directed mutagenesis was carried out using Quikchange<sup>TM</sup> site-directed  
128 mutagenesis kit (Stratagene, La Jolla, CA) for construction of E198A, A162G, and  
129 P217G. The nucleotide sequences of mutated MMP-7 genes were verified by a  
130 Shimadzu DNA sequencer DSQ-2000 (Kyoto).

131

132 2.3. *Fluorometric analysis of hydrolysis of MOCac-PLGL(Dpa)AR*

133

134 The MMP-7-catalyzed hydrolysis of MOCac-PLGL(Dpa)AR was initiated by  
135 mixing 1222  $\mu$ l of the reaction buffer, 20  $\mu$ l of the MMP-7 solution (625 nM), and 8  $\mu$ l  
136 of the substrate solution (234  $\mu$ M) dissolved in DMSO. The initial concentrations of  
137 enzyme, MOCac-PLGL(Dpa)AR, and DMSO were 10 nM, 1.5  $\mu$ M, and 0.64% (v/v),  
138 respectively. The reaction buffers were 50 mM acetate-NaOH buffer at pH 3.6-5.8, 50  
139 mM MES-NaOH buffer at pH 5.6-7.0, 50 mM HEPES-NaOH buffer at pH 6.8-8.6, and  
140 50 mM AMPSO-NaOH buffer at pH 8.6-10.4, each containing 10 mM CaCl<sub>2</sub>. The  
141 reaction was measured by following the increase in the fluorescence intensity at 393 nm

142 with excitation at 328 nm with a JASCO FP-777 fluorescence spectrophotometer  
143 (Tokyo, Japan). The peptide bond of Gly-L-Leu residues was cleaved by MMP-7, and  
144 the amount of the product MOCAC-PLG was estimated by the fluorescence intensity by  
145 comparison with the fluorescence intensity of an authentic MOCAC-PLG solution. The  
146 hydrolysis was carried out under pseudo-first order conditions, where the initial  
147 concentration of MOCAC-PLGL(Dpa)AR (1.5  $\mu\text{M}$ ) was much lower than  $K_m$  (60  $\mu\text{M}$ )  
148 [38]. The Michaelis-Menten equation is, then, expressed as Eq. 1.

149

$$150 \quad v_o = (k_{\text{cat}}/K_m)[E]_o[S]_o \quad (1)$$

151

152 where  $v_o$ ,  $k_{\text{cat}}$ ,  $[E]_o$ , and  $[S]_o$  mean the initial reaction rate, the molecular activity, the  
153 initial enzyme concentration, and the initial substrate concentration, respectively. The  
154 kinetic parameters, the intrinsic  $k_{\text{cat}}/K_m$ ,  $(k_{\text{cat}}/K_m)_o$ , and the proton dissociation constants  
155 ( $K_{e1}$  and  $K_{e2}$ ) for pH-dependence of the activity were calculated from Eq. 2 by a  
156 non-linear least squares regression method with Kaleida Graph Version 3.5 (Synergy  
157 Software, Essex, VT).

158

$$(k_{\text{cat}}/K_m)_{\text{obs}} = \frac{(k_{\text{cat}}/K_m)_o}{1 + \frac{[\text{H}^+]}{K_{e1}} + \frac{K_{e2}}{[\text{H}^+]}} \quad (2)$$

159

160 In this equation,  $(k_{\text{cat}}/K_m)_{\text{obs}}$  and  $[\text{H}]$  mean the  $k_{\text{cat}}/K_m$  value observed and the proton  
161 concentration, respectively, at the specified pH.

162

163 *2.4. Thermodynamic analysis of  $K_{e1}$  and  $K_{e2}$*

164

165 The enthalpy changes,  $\Delta H^\circ$ , of deprotonation were calculated from  $pK_e$  shifts using  
166 Eq. 3, known as the van't Hoff equation,

167

$$\frac{d(\ln K_e)}{dT} = \frac{\Delta H^\circ}{RT^2} \quad (3)$$

168

169 where  $T$  and  $R$  mean the absolute temperature in degrees Kelvin and the gas constant (=   
170  $8.314 \text{ J K}^{-1} \text{ mol}^{-1}$ ), respectively. When this equation is integrated, it is expressed as Eq.   
171 4,

172

$$-\log K_e = \frac{\Delta H^\circ}{2.303 RT} + A \quad (4)$$

173

174 where  $A$  means the constant of integration. Thus, a slope of a plot for  $pK_e$  values versus   
175  $1/T$  gives  $\Delta H^\circ$ .

176

177 *2.5. Titration of pH of amino-acid solution and thermodynamic analysis of proton*  
178 *dissociation constant of side chains of amino acids*

179

180 Amino acid was dissolved in water to be 10 mM for L-Asp, L-Glu, L-His, L-Cys,  
181 and L-Arg and 1 mM for L-Tyr and  $N^\alpha$ -acetyl-L-Lys. Titration was made with 50 or 100  
182  $\mu\text{l}$  of 2 M HCl or 2 M NaOH for each amino-acid solution (500 ml) incubated at 25, 35,  
183 or 45°C as follows: the L-Asp and L-Glu solutions were titrated with NaOH until pH  
184 reached 6.0. The L-His solution was titrated with HCl until pH reached 3.0. The L-Cys  
185 solution was titrated with HCl until pH reached 6.8. The L-Arg solution was titrated



186 with HCl until pH reached 9.8. The L-Tyr solution was titrated with HCl until pH  
 187 reached 7.5. The  $N^\alpha$ -acetyl-L-Lys solution was titrated with HCl until pH reached 9.2.

188 The following is the case with L-Glu, as an example. Based on the previous reports  
 189 that  $pK_a$  values of  $\alpha$ -COOH and  $\gamma$ -COOH of L-Glu at 25°C are around 2.0 and 4.0,  
 190 respectively [29-33], the course of a titration of L-Glu with NaOH from pH 2 to 6 can  
 191 be represented in the following schemes.

192



195

196 The degree of dissociation,  $\alpha$ , is defined as the following equation,

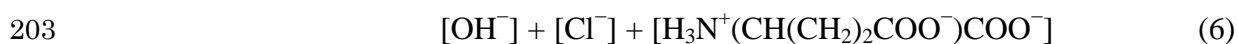
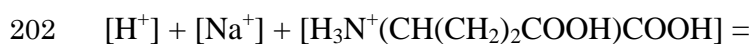
197

$$\alpha = \frac{2[H_3N^+(CH(CH_2)_2COO^-)COO^-] + [H_3N^+(CH(CH_2)_2COOH)COO^-]}{C} \quad (5)$$

198

199 where C means the initial concentration of L-Glu. The  $\alpha$  value increases up to 2 in the  
 200 course of the titration. The electric balance is given by the following equation.

201



204

205 Substituting Eq. 5 into Eq. 6 yields the following equation,

206

207

$$\alpha = \frac{C - [H^+] + [Na^+] - K_w/[H^+] - [Cl^-]}{C} \quad (7)$$

208

209 where  $K_w$  is ionic product. The  $\alpha$  at each pH was calculated from Eq. 7.  $K_{a1}$  and  $K_{a2}$ ,  
 210 which are defined as Eqs. 8 and 9, respectively, were calculated from Eq. 10 by a  
 211 non-linear least squares regression method with Kaleida Graph Version 3.5.

212

$$K_{a1} = \frac{[H^+] [H_3N^+(CH(CH_2)_2COOH)COO^-]}{[H_3N^+(CH(CH_2)_2COOH)COOH]} \quad (8)$$

213

$$K_{a2} = \frac{[H^+] [H_3N^+(CH(CH_2)_2COO^-)COO^-]}{[H_3N^+(CH(CH_2)_2COOH)COO^-]} \quad (9)$$

214

$$\alpha = \frac{2 + \frac{[H^+]}{K_{a2}}}{1 + \frac{[H^+]}{K_{a2}} + \frac{[H^+]^2}{K_{a1} K_{a2}}} \quad (10)$$

215

216  $\Delta H^\circ$  of deprotonation of side chains of L-Glu was calculated from  $pK_{a2}$  shift using Eq. 3.

217

### 218 3. Results

219

#### 220 3.1. $\Delta H^\circ$ values of deprotonation of side chains of amino acids

221

222 The wild-type MMP-7 was prepared as described in Materials and methods section.

223 Starting with 100 ml of *E. coli* cultures, 2 mg purified enzyme was recovered. Upon

224 SDS-PAGE under reducing conditions, each yielded a single band with a molecular

225 mass of 19 kDa (data not shown).

226 To determine  $\Delta H^\circ$  values of deprotonation of side chains of amino acids, we made  
227 a titration of pH of L-Asp, L-Glu, L-His, L-Cys, L-Tyr,  $N^\alpha$ -acetyl-L-Lys, and L-Arg  
228 solutions. The result with L-Glu is shown in Fig. 3, as an example. The degree of  
229 dissociation,  $\alpha$ , which is defined as Eq. 5, increased rapidly with an increase of pH from  
230 1.9 to 2.5, gradually with the increase from 2.5 to 3.8, and rapidly again with the  
231 increase from 3.8 to 4.5. The  $pK_{a1}$  and  $pK_{a2}$  were calculated by Eq. 10 to be  $2.1 \pm 0.1$   
232 and  $4.0 \pm 0.1$  for 25°C,  $2.2 \pm 0.1$  and  $4.1 \pm 0.1$  for 35°C, and  $2.3 \pm 0.1$  and  $4.2 \pm 0.1$  for  
233 45°C, respectively. The  $pK_{a1}$  was assigned to  $\alpha$ -carboxyl group, and the  $pK_{a2}$  was  
234 assigned to the side chain of L-Glu, based on the previous reports [29-33].  $\Delta H^\circ$  for the  
235  $pK_{a2}$  was calculated by the van't Hoff plot to be  $-23.6 \pm 5.8 \text{ kJ mol}^{-1}$  (inset of Fig. 3). All  
236 results are summarized in Table 1. The  $\Delta H^\circ$  of the side chains of L-Asp and L-Glu were  
237 negative, while those of the other five positive. The  $\Delta H^\circ$  of the side chains of L-Asp,  
238 L-His, and L-Cys were almost the same as the ones previously reported, which were  
239 determined by measuring the pH- and temperature-dependences of electromotive force  
240 of the battery containing amino acids or dipeptides in the cell ( $-6$  to  $6 \text{ kJ mol}^{-1}$  for L-Asp  
241 [29],  $29$ - $32 \text{ kJ mol}^{-1}$  for L-His [31], and  $24$ - $26 \text{ kJ mol}^{-1}$  for L-Cys [33]). On the other  
242 hand, the  $\Delta H^\circ$  of the side chains of the other four were substantially different from the  
243 ones previously reported ( $-6$  to  $6 \text{ kJ mol}^{-1}$  for L-Glu [29],  $25$ - $26 \text{ kJ mol}^{-1}$  for L-Tyr [31],  
244  $44$ - $55 \text{ kJ mol}^{-1}$  for L-Lys [31], and  $50$ - $52 \text{ kJ mol}^{-1}$  for L-Arg [31]).

245

246 *3.2.  $\Delta H^\circ$  of deprotonation of ionizable groups responsible for  $pK_{e1}$  and  $pK_{e2}$  of MMP-7*

247

248 According to Fig. 2 and Eq. 2, the pH dependence of  $k_{cat}/K_m$  results from the

249 association and dissociation of proton in the free MMP-7, but not the MMP-7 combined  
250 with substrate. The  $k_{\text{cat}}/K_{\text{m}}$  values of MMP-7 in the hydrolysis of  
251 MOCAc-PLGL(Dpa)AR in the pH range of 3.6-10.4 at 15, 25, 35, and 45°C were  
252 determined by Eq. 1 and are shown in Fig. 4. All plots showed bell-shaped curves. The  
253 plot at 15°C showed the widest active pH-range while that at 45°C showed the  
254 narrowest. The intrinsic  $k_{\text{cat}}/K_{\text{m}}$ ,  $(k_{\text{cat}}/K_{\text{m}})_o$ , and the  $\text{p}K_{\text{e}}$  values were determined by Eq. 2,  
255 which are summarized in Table 2. The  $(k_{\text{cat}}/K_{\text{m}})_o$  value was the lowest at 15°C and the  
256 highest at 45°C. Figure 5 shows van't Hoff plot for  $\text{p}K_{\text{e}1}$  and  $\text{p}K_{\text{e}2}$ .  $\Delta H^\circ$  of deprotonation  
257 were calculated to be  $-20.6 \pm 6.1 \text{ kJ mol}^{-1}$  for  $\text{p}K_{\text{e}1}$  and  $89.9 \pm 4.0 \text{ kJ mol}^{-1}$  for  $\text{p}K_{\text{e}2}$ .

258

### 259 *3.3. Estimation of the ionizable groups responsible for $\text{p}K_{\text{e}1}$ and $\text{p}K_{\text{e}2}$ of MMP-7*

260

261 By comparison with the  $\Delta H^\circ$  of MMP-7 ( $-20.6 \pm 6.1 \text{ kJ mol}^{-1}$  for  $\text{p}K_{\text{e}1}$  and  $89.9 \pm$   
262  $4.0 \text{ kJ mol}^{-1}$  for  $\text{p}K_{\text{e}2}$ ) with the  $\Delta H^\circ$  of side chains of amino acids (Table 1), glutamate  
263 residue was thought to be the ionizable group responsible for  $\text{p}K_{\text{e}1}$ , and arginine or  
264 lysine residue for  $\text{p}K_{\text{e}2}$ . This suggested that Glu198 is the ionizable group for  $\text{p}K_{\text{e}1}$  (Fig.  
265 1), as previously pointed out [4]. However, no arginine or lysine residues are found in  
266 the active site (Fig. 1). We therefore hypothesized that a protein-bound water is the  
267 ionizable group for  $\text{p}K_{\text{e}2}$ .

268

### 269 *3.4. Water molecules as the candidate for ionizable group responsible for $\text{p}K_{\text{e}2}$*

270

271 The hydroxamate (R-CO-NH-OH) peptide mimetic inhibitor, which binds  
272 covalently to the active-site zinc ion, is the first MMP inhibitor [40]. In the

273 MMP-7-hydroxamate inhibitor complex (Protein Data Bank no. 1MMQ) [4], we  
274 noticed two water molecules (W1 and W2) as the possible candidates for the ionizable  
275 group responsible for  $pK_{e2}$  (Fig. 1B), based on the following reasons: (i) W1 and W2 are  
276 located 2.7 Å far from each one of the two oxygen atoms of hydroxamate bound to the  
277 active site zinc ion; (ii) W1 binds to the main-chain nitrogen atom of Ala162, and W2  
278 binds to the main-chain carbonyl oxygen atom of Pro217. Ala162 is located at the fourth  
279  $\beta$ -sheet (Ala162-Ala164) of MMP-7, and Pro217 is located at the Met-turn  
280 (Pro211-Gly222). Both Ala162 and Pro217 are conserved among MMPs; and (iii) In the  
281 X-ray crystallographic structure of MMP-7 complexed with carboxylate inhibitor  
282 (1MMP) and sulfodiimine inhibitor (1MMR), the water molecules corresponding to W1  
283 and W2 are found [4].

284

### 285 3.5. Kinetic analysis of the MMP-7 variants

286

287 To see if the ionizable group responsible for  $pK_{e1}$  is Glu198, we constructed the  
288 MMP-7 variant, E198A. To explore the possibility that either W1 or W2 is the ionizable  
289 group responsible for  $pK_{e2}$ , we constructed the variants, A162G and P217G, assuming  
290 that the main-chain structure of MMP-7 could be changed by mutating Ala162 or  
291 Pro217 into glycine, which is the most flexible amino acid residue, and that such  
292 mutation alters  $pK_{e2}$  if the ionizable group responsible for  $pK_{e2}$  is located in the  
293 neighborhood of the site of mutation. The variants were produced in the *E. coli*  
294 expression system [38]. The pH-dependence of the  $k_{cat}/K_m$  of the wild-type MMP-7,  
295 E198A, A162G, and P217G in the hydrolysis of MOCAc-PLGL(Dpa)AR at 25°C is  
296 shown in Fig. 6, and the kinetic parameters are summarized in Table 3. E198A

297 completely lacked the activity. To see if it retained small  
298 MOCAC-PLGL(Dpa)AR-hydrolyzing activity, we made HPLC analysis [27]. No  
299 activity was detected in E198A even with the enzyme and substrate concentrations of 1  
300  $\mu\text{M}$  and 140  $\mu\text{M}$ , respectively, and the reaction time of 120 min (data not shown). On  
301 the other hand, the activity was detected in the wild-type enzyme with the enzyme and  
302 substrate concentrations of 1 nM and 140  $\mu\text{M}$ , respectively, and the reaction time of 10  
303 min (data not shown). This indicated that the activity of E198A, if any, was less than  
304 0.01% of that of the wild-type enzyme, suggesting that E198A completely lost the  
305 activity and that Glu198 is not the ionizable group responsible for  $\text{p}K_{\text{e}1}$ .

306 A162G and P217G retained the activity with the  $(k_{\text{cat}}/K_{\text{m}})_0$  values of 57% and 78%  
307 of that of the wild-type enzyme, respectively (Table 3). The  $\text{p}K_{\text{e}1}$  of A162G and P217G  
308 were  $4.9 \pm 0.1$  and  $5.3 \pm 0.1$ , being higher by  $0.3 \pm 0.2$  and  $0.7 \pm 0.2$  unit, respectively,  
309 than that of the wild-type enzyme ( $4.6 \pm 0.1$ ). The  $\text{p}K_{\text{e}2}$  of A162G and P217G were  $10.3$   
310  $\pm 0.1$  and  $10.0 \pm 0.1$ , being higher by  $0.6 \pm 0.2$  and  $0.3 \pm 0.2$  unit, respectively, than that  
311 of the wild-type enzyme ( $9.7 \pm 0.1$ ). These results indicated that the mutations of  
312 Ala162 $\rightarrow$ Gly and Pro217 $\rightarrow$ Gly affected the electrostatic environment of the ionizable  
313 groups responsible for not only  $\text{p}K_{\text{e}2}$  but also  $\text{p}K_{\text{e}1}$ .

314

## 315 **4. Discussion**

316

### 317 *4.1. Estimation of ionizable groups involved in the catalytic mechanism of MMP-7*

318

319 Browner et al. proposed that, based on the crystal structure of the complex of  
320 MMP-7 and its inhibitor, Glu198 is the ionizable group responsible for  $\text{p}K_{\text{e}1}$ : it functions

321 both as a base and an acid, deprotonating the zinc-bound water and transferring the  
322 proton to the leaving amine [4]. Cha et al. proposed that, based on the pH-dependence  
323 of the activity, Tyr219 is the ionizable group responsible for  $pK_{e2}$ : the ionized side chain  
324 of Tyr219 makes the active site of MMP-7 hydrophilic [25]. They also proposed that the  
325 zinc-bound water, but not Glu198, is the ionizable group responsible for  $pK_{e1}$ : the  
326 ionized zinc-bound water molecule attacks the carbonyl carbon of the scissile bond as a  
327 nucleophile [26]. We demonstrated that, based on the results with chemical modification  
328 [27] and site-directed mutagenesis [28], Tyr219 is not the ionizable group responsible  
329 for  $pK_{e2}$ .

330 Thermodynamic analysis in this study suggested that glutamate residue is the  
331 ionizable group for  $pK_{e1}$ , and that arginine or lysine residue is that for  $pK_{e2}$  (Tables 1  
332 and 2). The mutation of Glu198→Ala completely abolished activity (Table 3). We think  
333 that E198A has similar three-dimensional folds to the wild-type MMP-7 because the  
334 expression level and stability of E198A were similar to those of the wild-type MMP-7:  
335 starting from 100-ml culture, 2 mg purified E198A was obtained by the denaturation  
336 and refolding processes. Purified E198A was stable on storage at 4°C. On the other  
337 hand, some MMP-7 variants precipitated during the refolding process (K. Y. and K. I.,  
338 unpublished data). Although it is difficult to exclude a possibility that the loss of activity  
339 by the mutation Glu198→Ala does not result from the structural change, our result  
340 suggests that Glu198 is the ionizable group responsible for  $pK_{e1}$ . This agrees well with  
341 the previous reports that in MMP-1 [41], MMP-3 [42], and MMP-9 [43], the glutamate  
342 residue corresponding to Glu198 of MMP-7 is catalytically important. On the other  
343 hand, arginine and lysine residue were declined for the ionizable group for  $pK_{e2}$  because  
344 there are no lysine or arginine residues in the active site. We therefore proposed that a

345 protein-bound water is the ionizable group for  $pK_{e2}$ . We noticed two water molecules,  
346 Ala162-bound water (W1) and Pro217-bound water (W2), as the candidates for the  
347 ionizable group for  $pK_{e2}$ . The mutations of Ala162→Gly and Pro217→Gly altered not  
348 only  $pK_{e2}$  but also  $pK_{e1}$  values. This indicated that the mutations affected the  
349 electrostatic environment of the active site. To further explore our hypothesis, extensive  
350 site-directed mutagenesis study is required.

351

#### 352 4.2. Catalytic mechanism of MMP-7

353

354 Based on the results in this study, we propose the following catalytic mechanism of  
355 MMP-7 (Fig. 7). In free enzyme, Glu198 must be in its deprotonated state and the  
356 protein-bound water must be in its unionized state for catalysis (Fig. 7A). The Michaelis  
357 complex is formed when the carbonyl oxygen of the scissile bond binds the zinc ion.  
358 Zinc ion polarizes the carbonyl group of the scissile bond. Glu198 accepts a proton from  
359 the zinc-bound water (Fig. 7B). The tetrahedral complex is formed when the ionized  
360 zinc-bound water attacks the carbonyl carbon of the scissile bond, and then stabilized by  
361 the interaction between the carbonyl oxygen of the scissile bond and the oxygen of the  
362 protein-bound water in its unionized state (Fig. 7C). This stabilization does not occur  
363 when this protein-bound water is negatively charged. The amino product is released  
364 when Glu198 transfers the proton to the nitrogen of the scissile bond (Fig. 7D).

365  $pK_a$  of free water is 15.7. The above mechanism is consistent with the pH  
366 dependence of MMP-7 activity with  $pK_{e1}$  and  $pK_{e2}$  values of 4.0 and 9.8 if the  $pK_a$  of  
367 the protein-bound water greatly decreases. The zinc-bound water should be released in  
368 the MMP-7-hydroxamate inhibitor complex (Protein Data Bank no. 1MMQ) [4]



369 because hydroxamate (R-CO-NH-OH) binds to the zinc ion as the bidentate ligand.  
370 When the substrate coordinates to the zinc ion through the mono dentate ligand such as  
371 the carbonyl oxygen of the scissile bond, it still binds to the zinc ion. Therefore, it is  
372 thought that the  $pK_a$  of the zinc-bound water also greatly decreases. Considering the  
373 mechanism that the ionized zinc-bound water attacks the carbonyl carbon of the scissile  
374 bond (Fig. 7), it is thought that the ionizable group responsible for  $pK_{e2}$  is the  
375 protein-bound, but not zinc-bound, water.

376 It should be mentioned that in MMP-3, the protein-bound water involved in the  
377 catalytic mechanism was in its protonated state for catalysis, stabilizing the tetrahedral  
378 intermediate by coordinating the carbonyl oxygen of the scissile bond of the substrate  
379 [44]. In carboxypeptidase A, which belongs to Clan MC of zinc metalloproteinase, the  
380 ionizable group for  $pK_{e1}$  of 7 was assigned to the active-site glutamate residue, and that  
381 for  $pK_{e2}$  of 10 was assigned to the zinc-bound water molecule [45]. It was thought that  
382 the active-site glutamate residue functions as a general base while the zinc-bound water  
383 is in its unionized state, stabilizing the tetrahedral intermediate [45].

384

385 *4.3. Estimation of the ionizable groups involved in the catalytic mechanism of enzymes*  
386 *by  $\Delta H^\circ$  of deprotonation*

387

388  $pK_a$  of active-site residues can vary depending on their microenvironment. To our  
389 knowledge, the highest  $pK_a$  of the active-site glutamate residue is 8.4 in xylanase [46],  
390 suggesting that it is difficult to estimate the ionizable groups of enzymes only by their  
391  $pK_a$  values. In this study, we determined  $pK_a$  of side chains of L-Asp, L-Glu, L-His,  
392 L-Cys, L-Tyr, L-Lys, and L-Arg at 25-45°C by the pH titration of amino-acid solutions,

393 from which we calculated  $\Delta H^0$  of deprotonation. In the previous reports [29],  $\Delta H^0$  of  
394 side chains of L-Asp and L-Glu were the same (in the range of -6 to 6 kJ mol<sup>-1</sup>). In this  
395 study, they were different ( $-6.4 \pm 3.5$  kJ mol<sup>-1</sup> for L-Asp and  $-23.6 \pm 5.8$  kJ mol<sup>-1</sup> for  
396 L-Glu) (Table 1). Considering that the ionizable group for pK<sub>e1</sub> can be assigned to  
397 Glu198 by the  $\Delta H^0$  value ( $-20.6 \pm 6.1$  kJ mol<sup>-1</sup>), the  $\Delta H^0$  of side chains of amino acids  
398 presented in this study might be a powerful tool to estimate the ionizable groups  
399 involved in the catalytic mechanism of various enzymes.

400 In conclusion, we propose that Glu198 and unidentified protein-bound water are  
401 the ionizable groups involved in the catalytic mechanism of MMP-7. To identify the  
402 protein-bound water, site-directed mutagenesis study of MMP-7 is currently underway.

403

#### 404 **Acknowledgements**

405

406 This study was supported in part (K. I.) by Grants-in-Aid for Scientific Research (Nos.  
407 17380065 and 20380061) from the Japan Society of the Promotion of Science.

408

#### 409 **References**

410

411 [1] J.F. Woessner, Jr., Matrix metalloproteinases and their inhibitors in connective tissue  
412 remodeling. *FASEB J.* 5 (1991) 2145-2154.

413 [2] H. Nagase, J.F. Woessner, Jr., Matrix metalloproteinases. *J. Biol. Chem.* 274 (1999)  
414 21491-21494.

415 [3] J.F. Woessner, Jr., C.J. Taplin, Purification and properties of a small latent matrix  
416 metalloproteinase of the rat uterus. *J. Biol. Chem.* 263 (1988) 16918-16925.

- 417 [4] M.F. Browner, W.W. Smith, A.L. Castelhana, Matrilysin-inhibitor complexes:  
418 common themes among metalloproteinases. *Biochemistry* 34 (1995) 6602-6610.
- 419 [5] N.D. Rawlings, F.R., Morton, C.Y. Kok, J. Kong, A.J. Barrett, MEROPS: the  
420 peptidase database. *Nucleic Acids Res.* 36 (2008) D320-D325.
- 421 [6] W.-H. Yu, J.F. Woessner, Jr., Heparan sulfate proteoglycans as extracellular docking  
422 molecules for matrilysin (matrix metalloproteinase 7). *J. Biol. Chem.* 275 (2000)  
423 4183-4191.
- 424 [7] K. Yamamoto, S. Higashi, M. Kioi, J. Tsunozumi, K. Honke, K. Miyazaki, Binding  
425 of active matrilysin to cell surface cholesterol sulfate is essential for its  
426 membrane-associated proteolytic action and induction of homotypic cell adhesion. *J.*  
427 *Biol. Chem.* 281 (2006) 9170-9180.
- 428 [8] S. Higashi, M. Oeda, K. Yamamoto, K. Miyazaki, Identification of amino acid  
429 residues of matrix metalloproteinase 7 essential for binding to cholesterol sulfate. *J.*  
430 *Biol. Chem.* 283 (2008) 35735-35744.
- 431 [9] K. Yamamoto, K. Miyazaki, S. Higashi, Cholesterol sulfate alters substrate  
432 preference of matrix metalloproteinase-7 and promotes degradations of pericellular  
433 laminin-332 and fibronectin. *J. Biol. Chem.* 285 (2010) 28862-28873.
- 434 [10] C.C. Lynch, T. Vargo-Gogola, M.D. Martin, B. Fingleton, H.C. Crawford, L.M.  
435 Matrisian, Matrix metalloproteinase 7 mediates mammary epithelial cell tumorigenesis  
436 through the ErbB4 receptor. *Cancer Res.* 57 (2007) 6760-6767.
- 437 [11] H. Oneda, M. Shihara, K. Inouye, Inhibitory effects of green tea catechins on the  
438 activity of human matrix metalloproteinase 7 (matrilysin). *J. Biochem.* 133 (2003)  
439 571-576.
- 440 [12] Y. Muta, S. Oyama, T. Umezawa, M. Shimada, K. Inouye, Inhibitory effects of

441 lignans on the activity of human matrix metalloproteinase 7 (matrilysin). *J. Agric. Food*  
442 *Chem.* 52 (2004) 5888-5894.

443 [13] H. Oneda, K. Inouye, Interactions of human matrix metalloproteinase 7  
444 (matrilysin) with the inhibitors thiorphan and R-94138. *J. Biochem.* 129 (2001)  
445 429-435.

446 [14] H.I. Park, S. Lee, A. Ullah, Q. Cao, Q.X. Sang, Effects of detergents on catalytic  
447 activity of human endometase/matrilysin 2, a putative cancer biomarker. *Anal. Biochem.*  
448 396 (2010) 262-268.

449 [15] T. Crabbe, F. Willenbrock, D. Eaton, P. Hynds, A.F. Carne, G. Murphy, A.J.  
450 Docherty, Biochemical characterization of matrilysin. Activation conforms to the  
451 stepwise mechanisms proposed for other matrix metalloproteinases. *Biochemistry* 31  
452 (1992) 8500-8507.

453 [16] G.I. Goldberg, S.M. Wilhelm, A. Kronberger, E.A. Bauer, G.A. Grant, A.Z. Eisen,  
454 Human fibroblast collagenase. Complete primary structure and homology to an  
455 oncogene transformation-induced rat protein. *J. Biol. Chem.* 261 (1986) 6600-6605.

456 [17] B. Birkedal-Hansen, W.G. Moore, R.E. Taylor, A.S. Bhowan, H. Birkedal-Hansen,  
457 Monoclonal antibodies to human fibroblast procollagenase. Inhibition of enzymatic  
458 activity, affinity purification of the enzyme, and evidence of clustering epitopes in the  
459 NH<sub>2</sub>-terminal end of the activated enzyme. *Biochemistry* 27 (1988) 6751-6758.

460 [18] S.E. Whitham, G. Murphy, P. Angel, H.J. Rahmsdorf, B.J. Smith, A. Lyons, T.J.  
461 Harris, J.J. Reynolds, P. Herrlich, A.J. Docherty, Comparison of human stromelysin and  
462 collagenase by cloning and sequence analysis. *Biochem. J.* 240 (1986) 913-916.

463 [19] D. Muller, B. Quantin, M.C. Gesnel, R. Millon-Collard, J. Abecassis, R.  
464 Breathnach, The collagenase gene family in humans consists of at least four members.

465 Biochem. J. 253 (1988) 187-192.

466 [20] P. Devarajan, K. Mookhtiar, H. van Wart, N. Berliner, Structure and expression of  
467 the cDNA encoding human neutrophil collagenase. *Blood* 77 (1991) 2731-2738.

468 [21] H. Birkedal-Hansen, W.G. Moore, M.K. Bodden, L.J. Windsor, B. Birkedal-Hansen,  
469 A. DeCarlo, J.A. Engler, Matrix metalloproteinases: a review. *Crit. Rev. Oral Biol. Med.*  
470 4 (1993) 197-250.

471 [22] P. Basset, J.P. Bellocq, C. Wolf, I. Stoll, P. Hutin, J.M. Limacher, O.L. Podhajcer,  
472 M.P. Chenard, M.C. Rio, P. Chambon, A novel metalloproteinase gene specifically  
473 expressed in stromal cells of breast carcinomas. *Nature* 348 (1990) 699-704.

474 [23] T. Takino, H. Sato, E. Yamamoto, M. Seiki, Cloning of a human gene potentially  
475 encoding a novel matrix metalloproteinase having a C-terminal transmembrane domain.  
476 *Gene* 155 (1995) 293-298.

477 [24] Q.A. Sang, D.A. Douglas, Computational sequence analysis of matrix  
478 metalloproteinase. *J. Protein Chem.* 15 (1996) 137-160.

479 [25] J. Cha, M.V. Pedersen, D.S. Auld, Metal and pH dependence of heptapeptide  
480 catalysis by human matrilysin. *Biochemistry* 35 (1996) 15831-15838.

481 [26] J. Cha, D.S. Auld, Site-directed mutagenesis of the active site glutamate in human  
482 matrilysin: investigation of its role in catalysis. *Biochemistry* 36 (1997) 16019-16024.

483 [27] Y. Muta, H. Oneda, K. Inouye, Anomalous pH-dependence of the activity of human  
484 matrilysin (matrix metalloproteinase-7) as revealed by nitration and amination of its  
485 tyrosine residues. *Biochem. J.* 386 (2005) 263-270.

486 [28] Y. Muta, K. Inouye, Tyr219 of human matrix metalloproteinase 7 (MMP-7) is not  
487 critical for catalytic activity, but is involved in the broad pH-dependence of the activity.  
488 *J. Biochem.* in press

489 [29] J.T. Edsall, Dipolar ions and acid-base equilibria in: E.J. Cohn, J.T. Edsall (Eds.),  
490 Proteins, amino acids, and peptides as ions and dipolar ions, Hafner Publishing  
491 Company, New York and London, 1943, pp. 75-115.

492 [30] J.P. Geenstein, Studies of the peptides of trivalent amino acids. I. Titration  
493 constants of histidyl-histidine and of aspartyl-aspartic acid. J. Biol. Chem. 93 (1931)  
494 479-494.

495 [31] J.P. Greenstein, Studies of the peptides of trivalent amino acids. III. The apparent  
496 dissociation constants, free energy changes, and heats of ionization of peptides  
497 involving arginine, histidine, lysine, tyrosine, and aspartic and glutamic acids, and the  
498 behavior of lysine peptides toward nitrous acid. J. Biol. Chem. 101 (1933) 603-621.

499 [32] P.K. Smith, A.C. Taylor, E.R.B. Smith, Thermodynamic properties of solutions of  
500 amino acids and related substances. III. The ionization of aliphatic amino acids in  
501 aqueous solution from one to fifty degrees. J. Biol. Chem. 122 (1937) 109-123.

502 [33] R. Cecil, J.R. McPhee, A kinetic study of the reactions on some disulphides with  
503 sodium sulphite. Biochem. J. 60 (1955) 496-506.

504 [34] K. Hiromi, K. Takahashi, Z. Hamazu, S. Ono, Kinetic studies on gluc-amylase.  
505 III. The influence of pH on the rates of hydrolysis of maltose and panose. J. Biochem.  
506 59 (1966) 469-475.

507 [35] W.J. Zhu, M. Li, X.Y. Wang, Chemical modification studies on arginine kinase:  
508 essential cysteine and arginine residues at the active site. Int. J. Biol. Macromol. 41  
509 (2007) 564-571.

510 [36] M.Y. Kondo, D.N. Okamoto, J.A. Santos, M.A. Juliano, K. Oda, B. Pillai, M.N.  
511 James, L. Juliano, I.E. Gouvea, Studies on the catalytic mechanism of glutamic  
512 peptidase. J. Biol. Chem. 285 (2010) 21437-21445.

513 [37] C.G. Knight, F. Willenbrock, G. Murphy, A novel coumarin-labelled peptide for  
514 sensitive continuous assays of the matrix metalloproteinase. FEBS Lett. 296 (1992)  
515 263-266.

516 [38] Y. Muta, N. Yasui, Y. Matsumiya, M. Kubo, K. Inouye, Expression in *Escherichia*  
517 *coli*, refolding, and purification of the recombinant mature form of human matrix  
518 metalloproteinase 7 (MMP-7). Biosci. Biotechnol. Biochem. 74 (2010) 2151-2517.

519 [39] H. Oneda, K. Inouye, Refolding and recovery of recombinant human matrix  
520 metalloproteinase 7 (matrilysin) from inclusion bodies expressed by *Escherichia coli*. J.  
521 Biochem. 126 (1999) 905-911.

522 [40] M. Betz, P. Huxley, S.J. Davies, Y. Mushtaq, M. Pieper, H. Tschesche, W. Bode,  
523 F.X. Comis-Rüth, 1.8-Å crystal structure of the catalytic domain of human neutrophil  
524 collagenase (matrix metalloproteinase-8) complexed with a peptidomimetic  
525 hydroxamate primed-side inhibitor with a distinct selectivity profile. Eur. J. Biochem.  
526 247 (1997) 356-363.

527 [41] L.J. Windsor, M.K. Bodden, B. Birkedal-Hansen, J.A. Engler, H. Birkedal-Hansen,  
528 Mutational analysis of residues in and around the active site of human fibroblast-type  
529 collagenase. J. Biol. Chem. 269 (1994) 4033-4040.

530 [42] B. Arza, M. de Maeyer, J. Félez, D. Collen, H.R. Lijnen, H.R. (2001) Critical role  
531 of glutamic acid 202 in the enzyme activity of stromelysin-1 (MMP-3). Eur. J. Biochem.  
532 268 (2001) 826-831

533 [43] S. Rowsell, P. Hawtin, C.A. Minshull, H. Jepson, S.M. Brockbank, D.G. Barratt,  
534 A.M. Slater, W.L. McPheat, D. Waterson, A.M. Henney, R.A. Pauptit, Crystal structure  
535 of human MMP9 in complex with a reverse hydroxamate inhibitor. J. Mol. Biol. 319  
536 (2002) 173-181.

537 [44] V. Pelmeshnikov, P.E. Siegbahn, Catalytic mechanism of matrix  
538 metalloproteinases: two-layered ONIOM study. *Inorg. Chem.* 41 (2002) 5659-5666.

539 [45] K. Zhang, D.S. Auld, Structure of binary and ternary complexes of zinc and cobalt  
540 carboxypeptidase A as determined by X-ray absorption fine structure. *Biochemistry* 34  
541 (1995) 16306-16312.

542 [46] M.D. Joshi, G. Sidhu, I. Pot, G.D. Brayer, S.G. Withers, L.P. McIntosh, Hydrogen  
543 bonding and catalysis: a novel explanation for how a single amino acid substitution can  
544 change the pH optimum of a glycosidase. *J. Mol. Biol.* 299 (2000) 255-279.

545



546 **Figure Legends**

547

548 Fig. 1. Structure of MMP-7. The MMP-7-hydroxamate inhibitor complex (Protein Data  
549 Bank no. 1MMQ) [4] was drawn using Swiss-Pdb Viewer 4.0. The active-site zinc ion is  
550 shown as a sphere. (A) Overall structure. Peptide chain is represented by a ribbon. The  
551 side chains of Glu198, Tyr193, Tyr216, and Tyr219 and the hydroxamate inhibitor are  
552 shown as a stick. (B) Close-up view of the active site. The side chains of Glu198 and  
553 Tyr219, the main and side chains of Ala162 and Pro217, and the two water molecules  
554 (W1 and W2) are shown as a ball and stick. The hydroxamate inhibitor is shown as a  
555 wire with the nearest two oxygen atoms to the active-site zinc ion as a ball. The number  
556 indicates that of the amino acid residues.

557

558 Fig. 2. Reaction scheme for the pH-dependence of MMP-7 activity with two ionizable  
559 groups involved in enzyme activity. E, S, H, and P denote MMP-7, the substrate, proton,  
560 and the product, respectively.  $K_{e1}$  and  $K_{e2}$  are proton dissociation constants of the  
561 ionizable groups of the free MMP-7, respectively, and  $K_{es1}$  and  $K_{es2}$  are proton  
562 dissociation constants of the MMP-7 combined with substrate, respectively [27,34].

563

564 Fig. 3. Titration curve of pH of L-Glu solution. The titration was carried out at 25 (open  
565 circle), 35 (open square), and 45°C (open triangle). The degree of dissociation of L-Glu  
566 at each pH was calculated by Eq. 7. The  $pK_{a1}$  and  $pK_{a2}$  were calculated by Eq. 10, which  
567 were  $2.1 \pm 0.1$  and  $4.0 \pm 0.1$  for 25°C,  $2.2 \pm 0.1$  and  $4.1 \pm 0.1$  for 35°C, and  $2.3 \pm 0.1$   
568 and  $4.2 \pm 0.1$  for 45°C, respectively. Inset shows van't Hoff plot for  $pK_{a2}$  of L-Glu.  
569 Enthalpy change,  $\Delta H^\circ$ , of deprotonation was calculated to be  $-23.6 \pm 5.8 \text{ kJ mol}^{-1}$ . One  
570 of the representative data is shown.

571

572 Fig. 4. Effect of pH on the wild-type MMP-7-catalyzed hydrolysis of  
573 MOCAc-PLGL(Dpa)AR. The reaction was carried out at 15 (open circle), 25 (open  
574 square), 35 (open triangle), and 45°C (open diamond), each with the initial enzyme and  
575 substrate concentrations of 10 nM and 1.5 μM, respectively. The relative  $k_{cat}/K_m$  is  
576 defined as the ratio of the  $k_{cat}/K_m$  at the indicated pH to that at the optimal pH ( $1.63 \times$   
577  $10^{-4} \text{ M}^{-1} \text{ s}^{-1}$  at pH 6.8 for 15°C,  $4.01 \times 10^{-4} \text{ M}^{-1} \text{ s}^{-1}$  at pH 6.8 for 25°C,  $5.39 \times 10^{-4} \text{ M}^{-1} \text{ s}^{-1}$   
578 at pH 6.6 for 35°C, and  $7.77 \times 10^{-4} \text{ M}^{-1} \text{ s}^{-1}$  at pH 6.0 for 45°C). Error bars indicate SD  
579 values. One of the representative data is shown.

580

581 Fig. 5. van't Hoff plot for  $pK_e$  of MMP-7.  $pK_{e1}$  (A) and  $pK_{e2}$  (B) values of MMP-7 were  
582 plotted against the reciprocal of the absolute temperature. Error bars indicate SD values.  
583 Enthalpy change,  $\Delta H^\circ$ , of deprotonation was calculated from the slope: (A)  $-20.6 \pm 6.1$   
584  $\text{kJ mol}^{-1}$ ; (B)  $89.9 \pm 4.0 \text{ kJ mol}^{-1}$ . One of the representative data is shown.

585

586 Fig. 6. Effect of pH on the MMP-7 variants-catalyzed hydrolysis of  
587 MOCAc-PLGL(Dpa)AR at 25°C. The reaction was carried out with the wild-type  
588 MMP-7 (open circle), A162G (open square), and P217G (open triangle). The initial  
589 enzyme and substrate concentrations were 10 nM and 1.5 μM, respectively. The relative  
590  $k_{cat}/K_m$  is defined as the ratio of the  $k_{cat}/K_m$  at the indicated pH to that at the optimal pH  
591 ( $4.01 \times 10^{-4} \text{ M}^{-1} \text{ s}^{-1}$  at pH 6.8 for the wild-type MMP-7,  $2.46 \times 10^{-4} \text{ M}^{-1} \text{ s}^{-1}$  at pH 6.8 for  
592 A162G, and  $3.18 \times 10^{-4} \text{ M}^{-1} \text{ s}^{-1}$  at pH 7.0 for P217G). Error bars indicate SD values. One  
593 of the representative data is shown.

594

595 Fig. 7. Proposed mechanism for the MMP-7-catalyzed cleavage of peptides. See the text

596 for details.

597

A

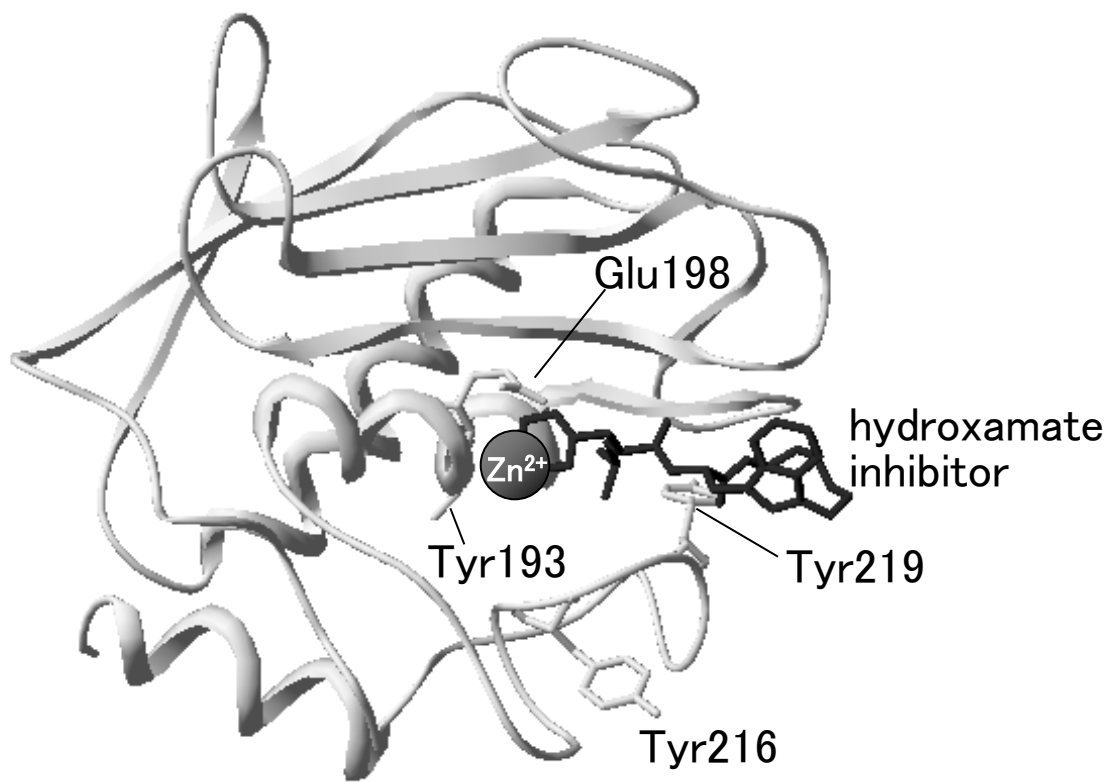


Fig. 1

B

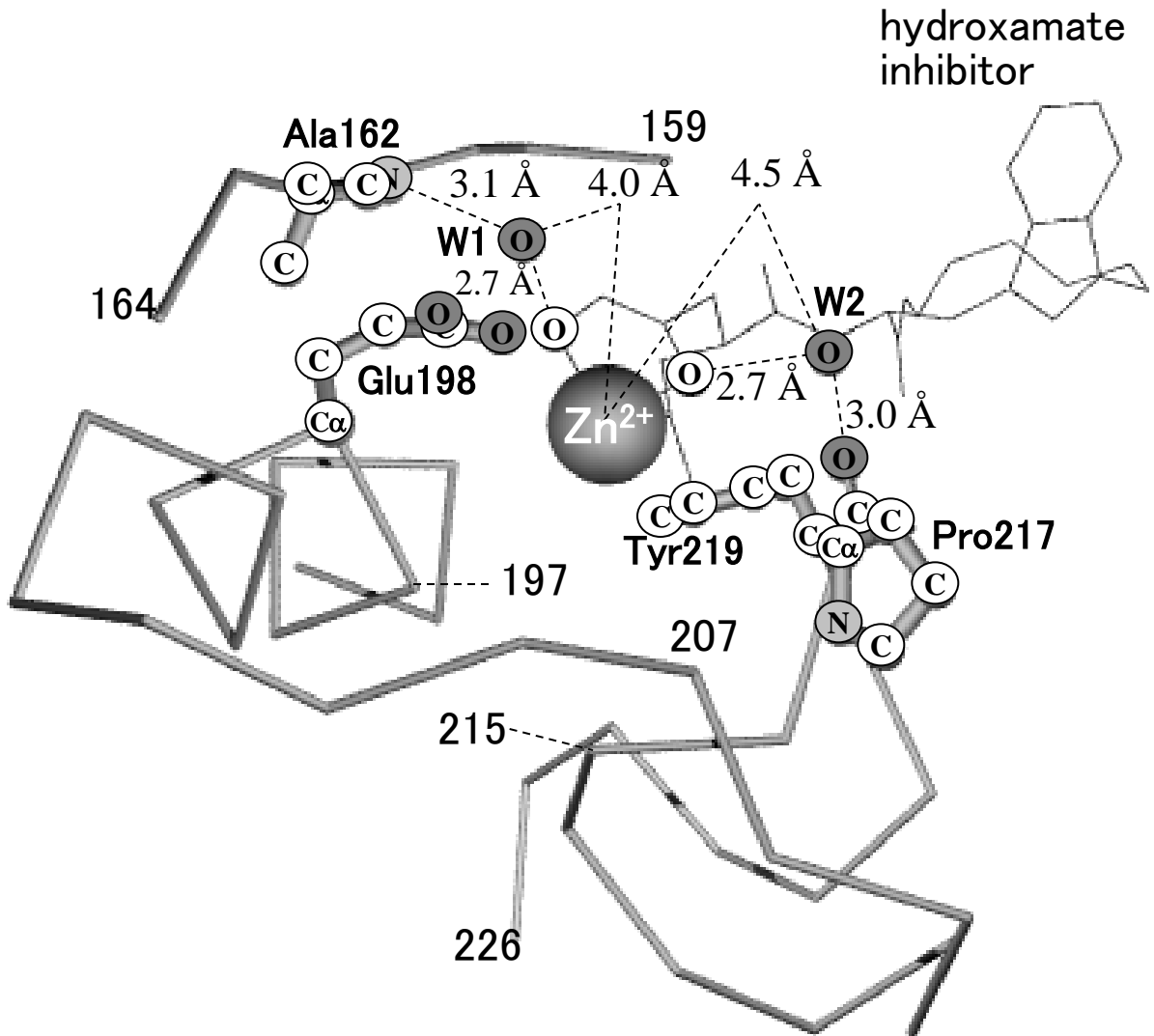
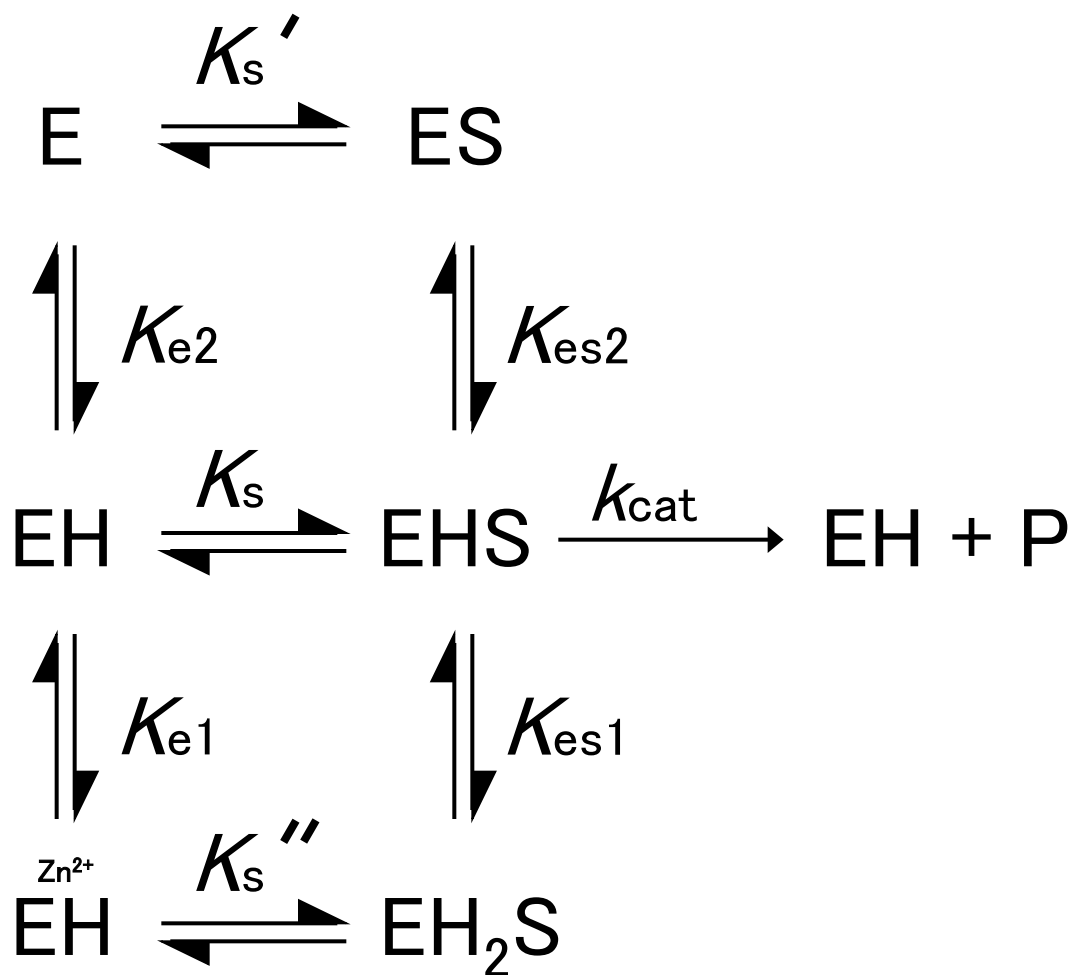


Fig. 1



2

Fig. 2

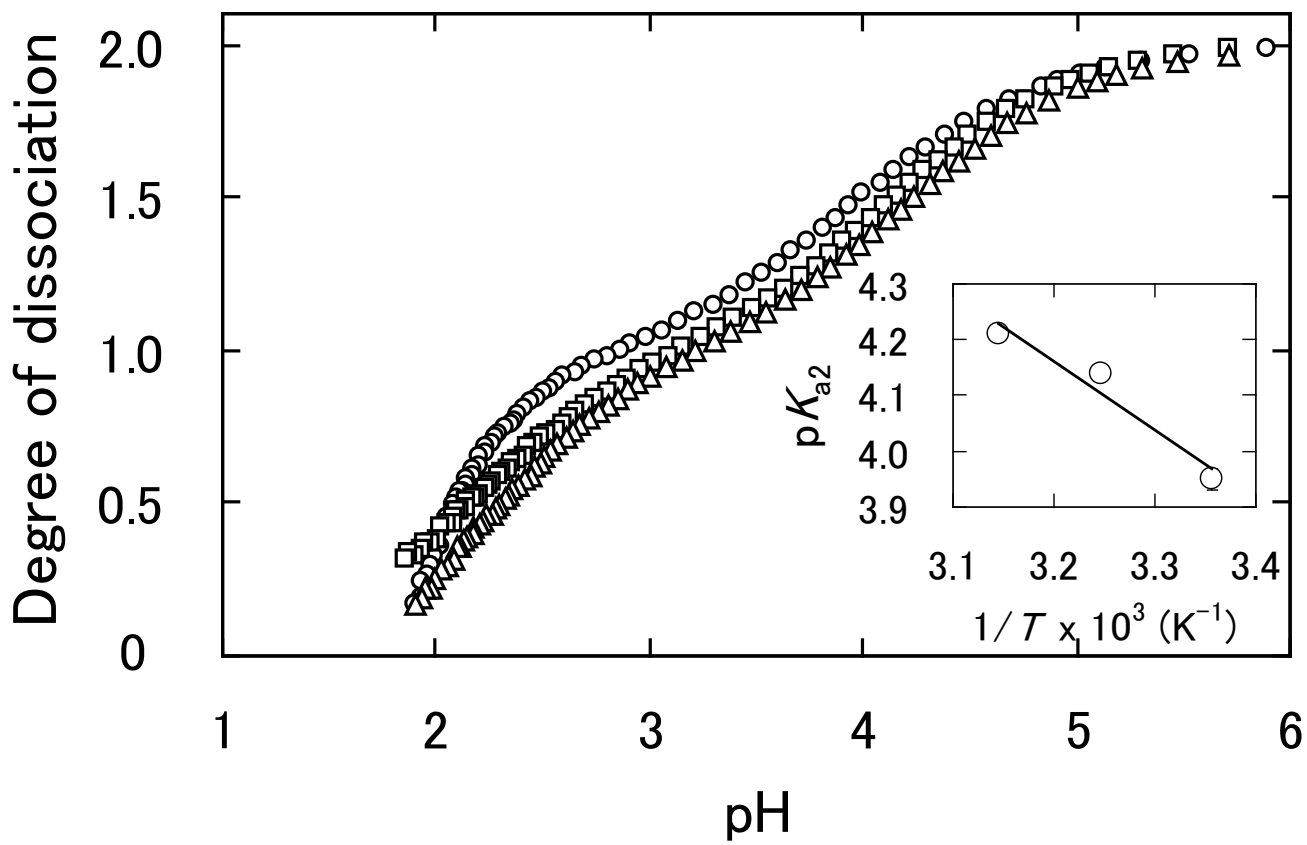


Fig. 3

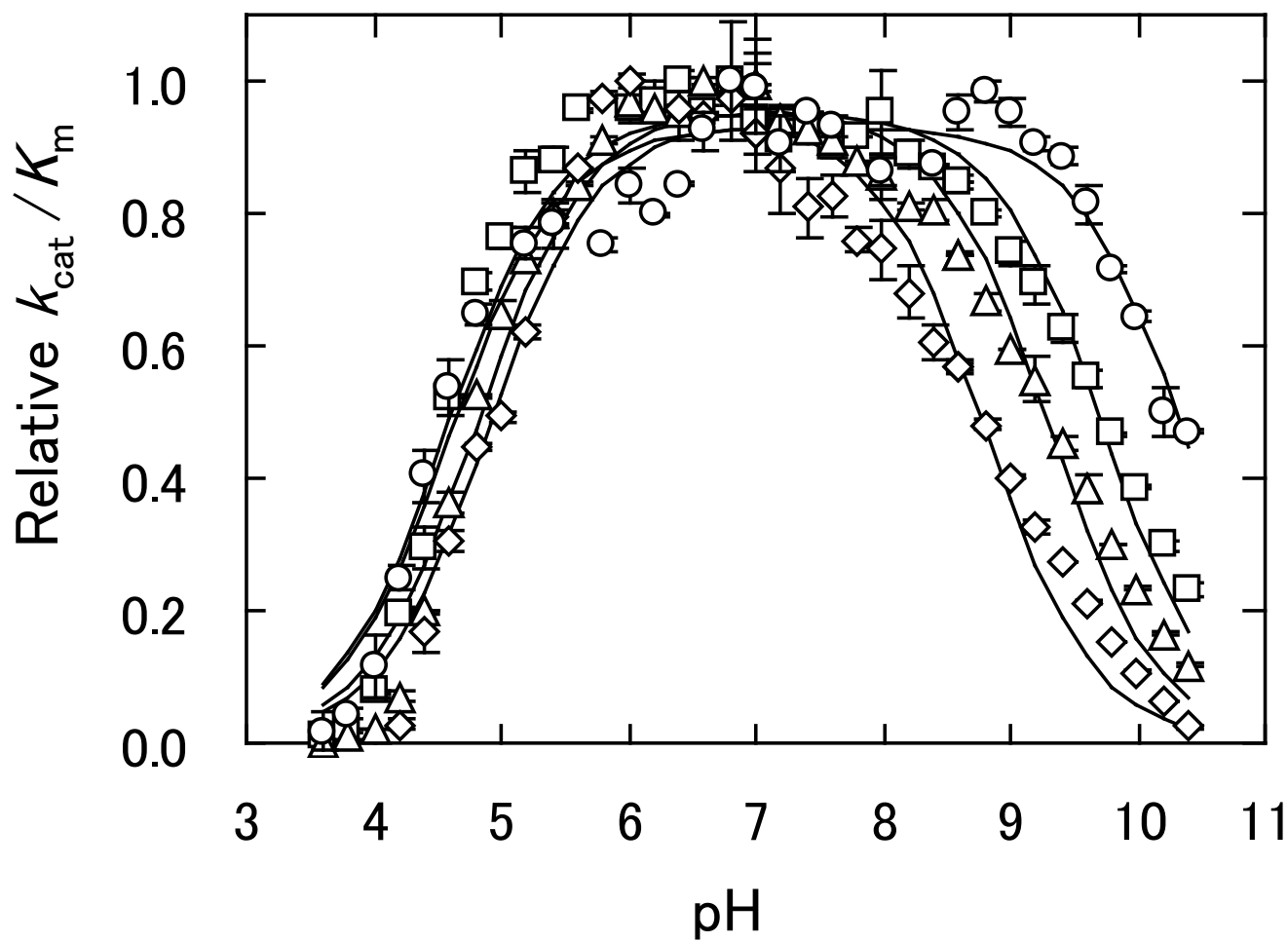


Fig. 4



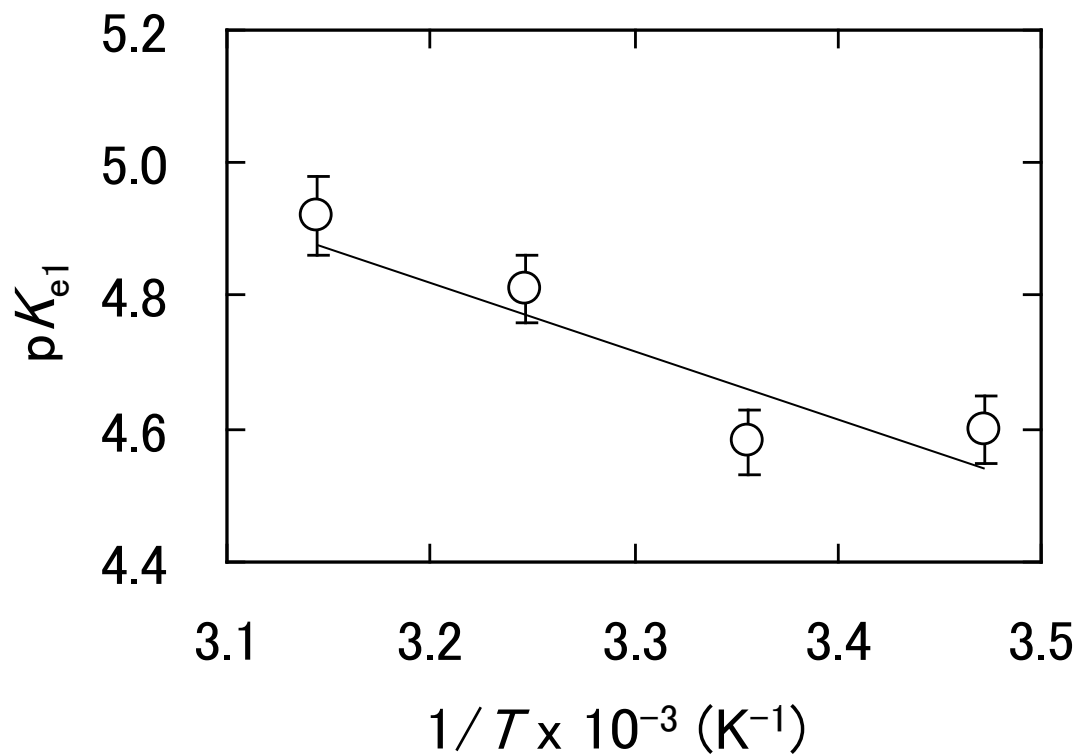
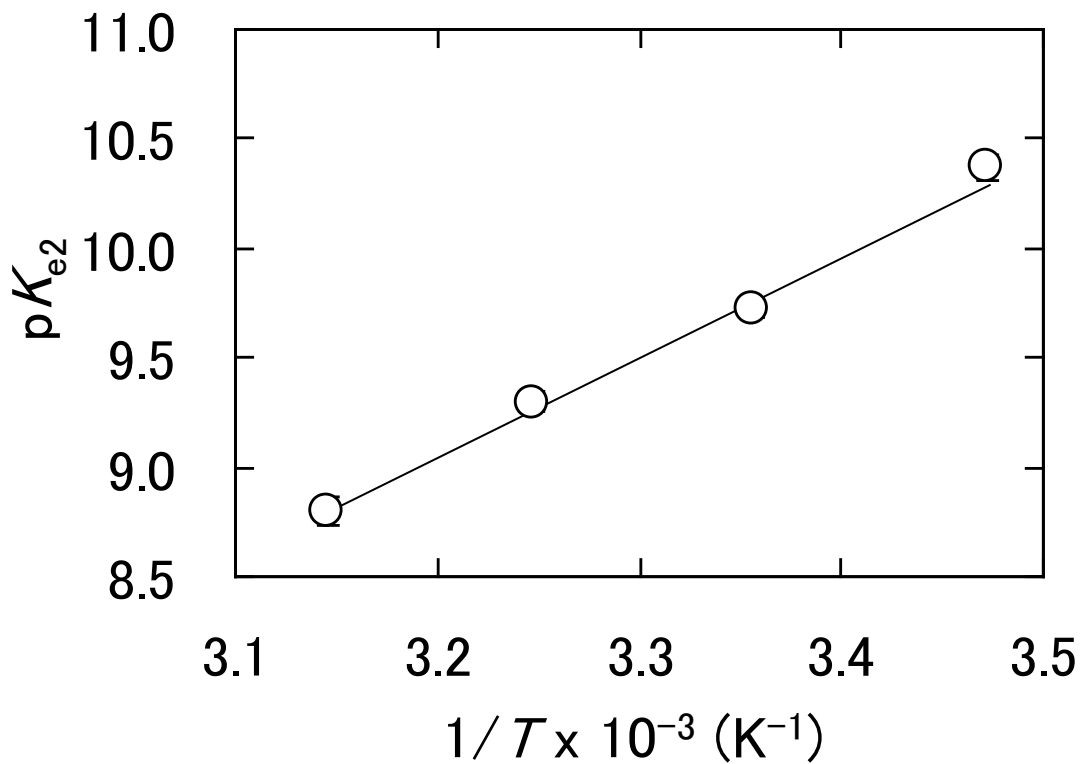
**A****B**

Fig. 5

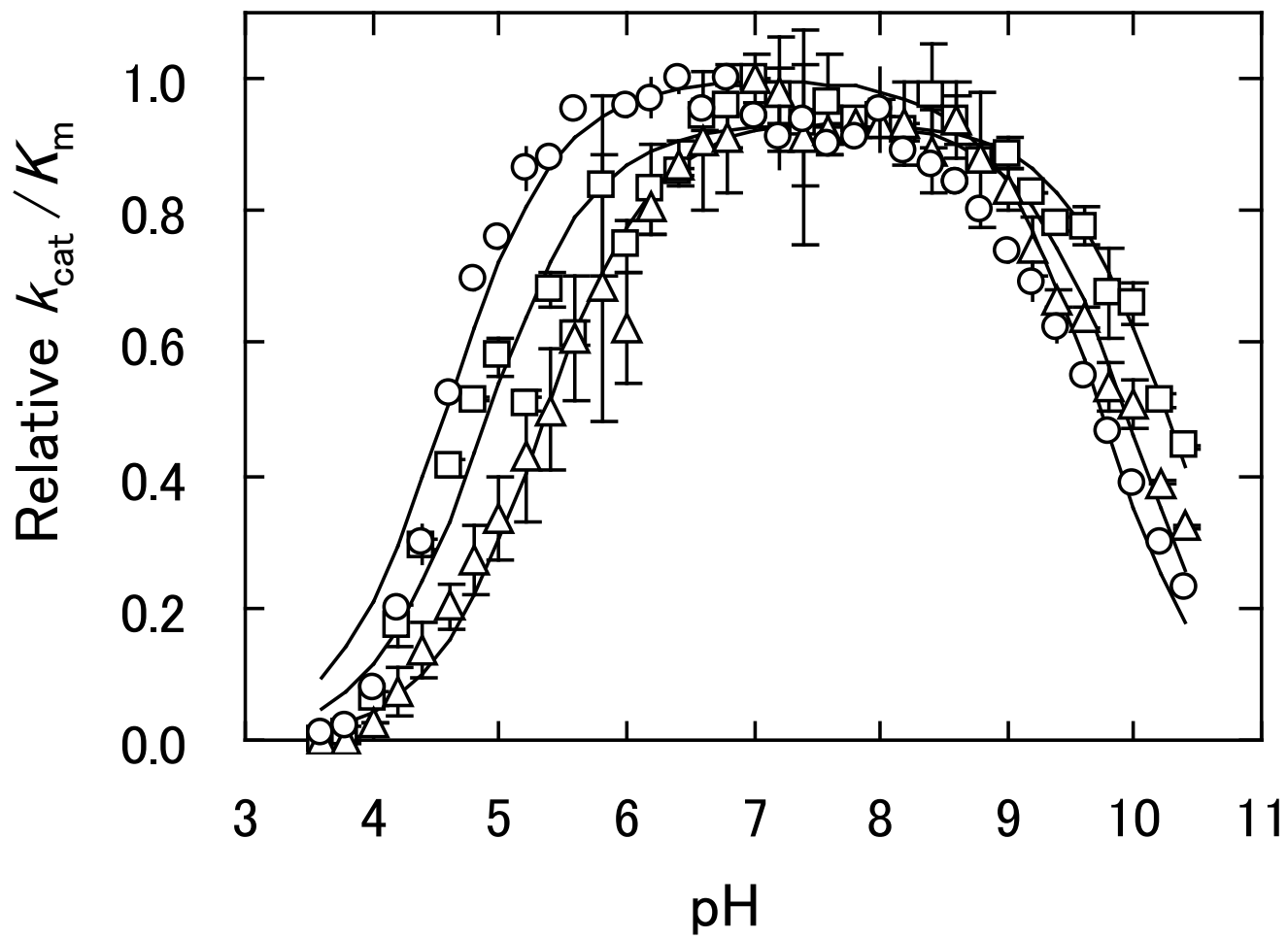


Fig. 6

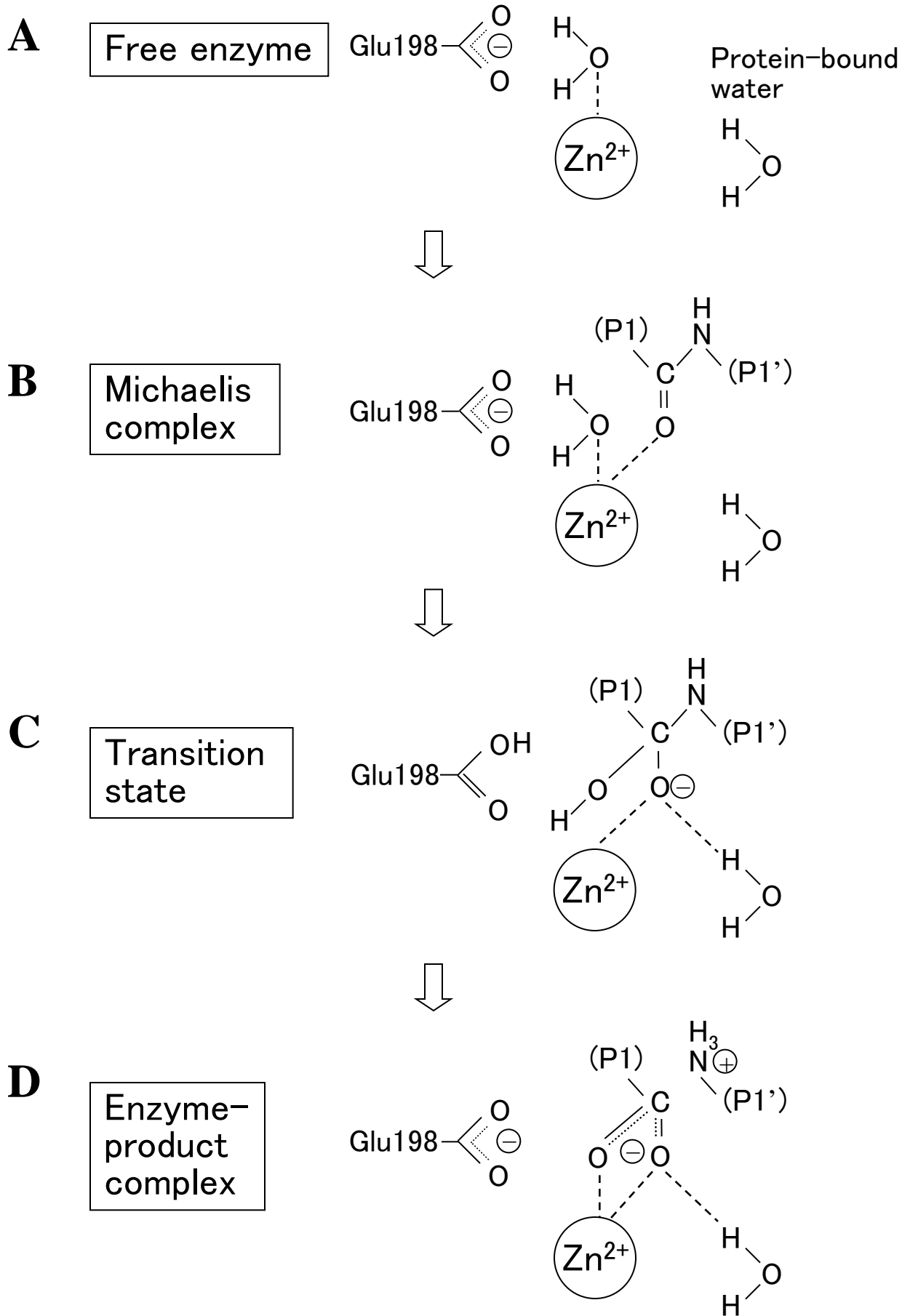


Fig. 7